

UC Irvine

UC Irvine Previously Published Works

Title

KCNQ5 Potassium Channel Activation Underlies Vasodilation by Tea

Permalink

<https://escholarship.org/uc/item/1070g8qs>

Journal

Cellular Physiology and Biochemistry, 55(S3)

ISSN

1015-8987

Authors

Redford, Kaitlyn E

Rognant, Salomé

Jepps, Thomas A

et al.

Publication Date

2021-03-06

DOI

10.33594/000000337

Copyright Information

This work is made available under the terms of a Creative Commons Attribution-NonCommercial-NoDerivatives License, available at

<https://creativecommons.org/licenses/by-nc-nd/4.0/>

Peer reviewed



Published in final edited form as:

Cell Physiol Biochem. 2021 March 06; 55(Suppl 3): 46–64. doi:10.33594/000000337.

KCNQ5 Potassium Channel Activation Underlies Vasodilation by Tea

Kaitlyn E. Redford^a, Salomé Rognant^b, Thomas A. Jepps^b, Geoffrey W. Abbott^a

^aBioelectricity Laboratory, Department of Physiology and Biophysics, School of Medicine, University of California, Irvine, CA, USA,

^bDepartment of Biomedical Sciences, Vascular Biology Group, Panum Institute, University of Copenhagen, Copenhagen, Denmark

Abstract

Background/Aims: Tea, produced from the evergreen *Camellia sinensis*, has reported therapeutic properties against multiple pathologies, including hypertension. Although some studies validate the health benefits of tea, few have investigated the molecular mechanisms of action. The KCNQ5 voltage-gated potassium channel contributes to vascular smooth muscle tone and neuronal M-current regulation.

Methods: We applied electrophysiology, myography, mass spectrometry and *in silico* docking to determine effects and their underlying molecular mechanisms of tea and its components on KCNQ channels and arterial tone.

Results: A 1% green tea extract (GTE) hyperpolarized cells by augmenting KCNQ5 activity >20-fold at resting potential; similar effects of black tea were inhibited by milk. In contrast, GTE had lesser effects on KCNQ2/Q3 and inhibited KCNQ1/E1. Tea polyphenols epicatechin gallate (ECG) and epigallocatechin-3-gallate (EGCG), but not epicatechin or epigallocatechin, isoform-selectively hyperpolarized KCNQ5 activation voltage dependence. *In silico* docking and mutagenesis revealed that activation by ECG requires KCNQ5-R212, at the voltage sensor foot. Strikingly, ECG and EGCG but not epicatechin KCNQ-dependently relaxed rat mesenteric arteries.

Conclusion: KCNQ5 activation contributes to vasodilation by tea; ECG and EGCG are candidates for future anti-hypertensive drug development.

This article is licensed under the Creative Commons Attribution-NonCommercial-NoDerivatives 4.0 International License (CC BY-NC-ND). Usage and distribution for commercial purposes as well as any distribution of modified material requires written permission.

Dr. Geoffrey W. Abbott, Bioelectricity Laboratory, Dept. of Physiology and Biophysics, Irvine Hall 249, School of Medicine Health Sciences Road, University of California, Irvine, CA 92697 (USA), Tel. +1 949 824 3269, abbottg@hs.uci.edu.

Author Contributions

KER prepared green tea extracts, performed the oocyte experiments and analyses, prepared most of the figure panels, and wrote part of the manuscript. SR conducted myography studies and analyzed data. TAJ analyzed and interpreted myography data, prepared the myography figure and edited the manuscript. GWA conceived the study, performed *in silico* structural analyses, helped write the manuscript and helped prepare the figures.

Statement of Ethics

Animals were used in accordance with Directive 2010/63EU on the protection of animals used for scientific purposes, approved by the national ethics committee, Denmark.

Disclosure Statement

The authors have no conflicts to disclose.

Keywords

Green tea; Hypotensive; I_{KS} ; KCNQ; Kv7; Polyphenol

Introduction

Since its initial use in China over 4000 years ago, tea has become one of the most commonly consumed beverages worldwide, second only to water [1]. The leaves of the evergreen species *Camellia sinensis* are used to make the most prevalent caffeinated teas (Fig. 1A). Since they are produced from the same plant, the differences between tea varieties (green, oolong, and black) are due to leaf fermentation levels (unfermented, partially fermented, and fully fermented, respectively), which impart the characteristic properties and flavors of the teas [1].

Though there is evidence of health benefits conferred by all tea produced by *Camellia sinensis* [2], green tea is the most studied as it has the highest antioxidant properties [3]. *In vivo* and *in vitro* studies show green tea extract inhibits carcinogenesis, as well as reduces hypertension and risk of heart disease [4–7]. However, the mechanism behind these therapeutic properties remains incompletely resolved. Medicinal plants contain bioactive compounds that either act independently or synergize to produce therapeutic results. The leaves of *Camellia sinensis* contain polyphenols belonging to the catechin family—specifically epicatechin (EC), epigallocatechin (EGC), epicatechin gallate (ECG), and epigallocatechin-3-gallate (EGCG) [1]. These catechins are known for their antioxidant properties and are thought to convey the therapeutic benefits of tea, with some studies showing anticancer and cardiovascular health benefits [8]. The fermentation process of the leaves that results in the different tea varieties causes the oxidization of catechins, resulting in green tea containing a higher concentration of catechins [3].

We recently showed that herbs with hypotensive properties were unified in their ability to activate the vascular and neuronal voltage-gated potassium (Kv) channel, KCNQ5 [9]. KCNQ5 belongs to the KCNQ (Kv7) subfamily of voltage-gated potassium channels, which in the human genome is composed of five genes (*KCNQ1–5*). Each gene encodes six transmembrane domains (S1–S4 compose the voltage sensing domain, and S5–S6 form the pore module) (Fig. 1B). Homo- or heterotetramers form to produce active channels. Ancillary peptides, such as KCNEs, are also incorporated *in vivo* to modulate the channel properties (Fig. 1C) [10, 11]. Homomeric KCNQ1, for example, is not known to be expressed *in vivo* without a KCNE modifier subunit [12]. The KCNQ1/E1 co-assembly produces the slow-acting cardiac ventricular repolarization current (I_{KS}) [13].

KCNQ2/Q3 and KCNQ3/Q5 α subunit heterotetramers, and possibly homomeric KCNQ2, KCNQ3, and/or KCNQ5, are important for generating the muscarinic receptor-inhibited Kv current (M-current) that regulates neuronal firing [14–17]. KCNQ4, expressed in auditory neurons and hair cells, is required for hearing [18]. KCNQ1, KCNQ4, and KCNQ5 expressed in vascular and non-vascular smooth muscle cells regulate the resting membrane potential of these cells, thereby controlling their contractility [19]. In the vasculature, KCNQ4/Q5 heteromers are involved in controlling arterial tone at rest, causing

vasoconstriction when these channels are blocked [20]. Due to their roles in a variety of physiological processes and different expression patterns, KCNQ channels are both linked to various inherited disease states and a potential drug target for a variety of diseases [12, 21].

Here, we hypothesized that KCNQ5 activation might underlie purported hypotensive properties of tea. We report that green and black tea extracts strongly and isoform-selectively activate KCNQ5. Screening the common catechins in tea, we found that ECG and EGCG selectively activate KCNQ5, making them potential candidates for future medicinal chemistry optimization and drug development for hypertension and even KCNQ5 loss-of-function encephalopathy.

Materials and Methods

Preparation of extracts and compounds

A methanolic extraction (80% methanol/20% water) was performed on 5 bags of Organic Green Tea sourced from Trader Joe's (Irvine, CA, US) and on the contents of 5 PG Tips black teabags sourced from [Amazon.com](https://www.amazon.com). Each methanol mixture (100 ml) was occasionally inverted over a 48-hour incubation at room temperature (20–25°C). After filtering with Whatman filter paper #1 (Whatman, Maidstone, UK), the methanol was evaporated off over 24 hours at room temperature (20–25°C) in a fume hood. The remaining extract was centrifuged for 10 minutes at 23°C, 4000 RCF to remove any remaining particulates and stored at –20°C. For electrophysiological recordings, the extract was thawed and diluted to 1:100 in bath solution (see below) immediately before use. EC and ECG were solubilized in bath solution to a concentration of 1 mM (more concentrated solutions would require a different solvent) and diluted to appropriate concentrations before use. Likewise, a 1 mM solution of EGCG was prepared in bath solution and used fresh, with the remaining stock solution heated at 35°C for approximately 3 hours and stored at 4°C for four weeks before use.

Channel subunit cRNA preparation and *Xenopus laevis* oocyte injection

cRNA transcripts encoding ion channel subunits (KCNQ1, KCNQ2, KCNQ3, KCNQ4, KCNQ5, and KCNE1) were generated using *in vivo* transcription with the mMessage mMachine kit (Thermo Fisher Scientific) from linearized cDNA sub-cloned into plasmids with *Xenopus laevis* β -globin 5' and 3' UTRs flanking the coding region. The mutant KCNQ5 cDNA was generated by site-directed mutagenesis using the QuikChange kit (Stratagene, San Diego, CA) and transcribed as described above. The cRNAs (2–20ng) were injected into defolliculated stage V and VI *Xenopus laevis* oocytes (Xenoocyte, Dexter, MI, US). The oocytes were stored at 16°C in ND96 oocyte storage solution containing penicillin and streptomycin, with daily washing, for 2–4 days prior to two-electrode voltage-clamp (TEVC) recording.

Two-electrode voltage clamp (TEVC)

We performed TEVC at room temperature with an OC-725C amplifier (Warner Instruments, Hamden, CT) and pClamp10 software (Molecular Devices, Sunnyvale, CA). Oocytes were placed in a small-volume oocyte bath (Warner). We solubilized tea polyphenols (Sigma) and

tea extract directly in bath solution (in mM, 96 NaCl, 4 KCl, 1 MgCl₂, 1 CaCl₂, 10 HEPES; pH 7.6). We introduced tea extract/compounds via gravity perfusion (1ml/minute for 3 minutes) before recording with pipettes of 1–3 MΩ resistance when filled with 3 M KCl. For intracellular ECG injection, we recorded a control voltage family, then immediately injected 50 nl of 2 mM ECG into each oocyte, giving an approximate intracellular ECG concentration of 100 μM assuming 1 μl oocyte volume. The post-ECG voltage family was recorded 20 minutes after ECG injection.

Recordings were performed with voltage pulses between –80 mV and +40 mV at 20 mV increments for the prepulse from a holding potential of –80 mV and then holding at –30 mV for the tail pulse before repolarizing to –80 mV (see figures for protocols). Clampfit (Molecular Devices) and GraphPad Prism software (GraphPad, San Diego, CA, USA) were used to analyze data and produce figures. Raw and normalized tail currents were fitted with a single Boltzman function:

$$g = \frac{(A_1 - A_2)}{\left\{1 + \exp\left[\frac{V_{1/2} - V}{V_s}\right]\right\}} y + A_2 \quad \text{Equation 1:}$$

where g is the normalized tail conductance, A_1 is the initial value at $-\infty$, A_2 is the final value at $+\infty$, $V_{1/2}$ is the half-maximal voltage of activation and V_s the slope factor. We fitted activation and deactivation kinetics with single exponential functions.

Chemical structures and silico docking

We plotted and viewed chemical structures and electrostatic surface potential using Jmol, an open-source Java viewer for chemical structures in 3D: <http://jmol.org/>. For *in silico* ligand docking predictions of binding to KCNQ5 we performed unguided docking of ECG using SwissDock with CHARMM forcefields [22, 23] and a chimeric human neuronal KCNQ/*Xenopus* KCNQ1 cryo-electron microscopy model as previously described [24].

Ultra-Performance Liquid chromatography-mass spectrometry (UPLC-MSe)

A 30-minute UPLC-MSe protocol was performed using a Waters Synapt G2 with a flow rate of 0.1 mL/min. Starting with 98% solution A (0.1% formic acid in water) and 2% solution B (100% acetonitrile), the protocol linearly ramps to 70% solution A and 30% solution B for the first 20 minutes. From minutes 20–25, another linear ramp begins until reaching 3% solution A and 97% solution B, which is held for 2.5 additional minutes; after which, a 1.5 minute linear ramp brings solution A back to 98% and solution B to 2%, which is held until the end of the run. MSe continuum data was obtained in positive mode with the analyzer mode set to resolution, with a mass range of 105 Da to 2000 Da, scanning every 250ms. The low energy was 6V, high energy ramped from 20–45V, with the cone voltage being 30V. The temperature was kept at 110°C. The resulting chromatograms were analyzed using MassLynx. The spectra for the prominent peaks was analyzed and searched using the Human Metabolomics Database (HMDB), protonated under positive mode with a 0.05 Da molecular weight tolerance. The 459.110 Da peak was identified as HMDB0003153 (EGCG).

Mesenteric artery myography

Male wistar rats, 12 weeks old (Janvier Labs, France) were euthanized by cervical dislocation and used in accordance with Directive 2010/63EU on the protection of animals used for scientific purposes, approved by the national ethics committee, Denmark. Rats were group-housed with regular 12-hour light/dark cycles, in clear plastic containers with *ad libitum* access to food and water and underwent at least one week of habituation. The intestines were removed, and third-order mesenteric arteries were dissected in ice-cold physiological saline solution containing (in mM): 121 NaCl, 2.8 KCl, 1.6 CaCl₂, 25 NaHCO₃, 1.2 KH₂HPO₄, 1.2 MgSO₄, 0.03 EDTA, and 5.5 glucose. Segments, 2 mm in length, of mesenteric artery were mounted on 40 µm stainless steel wires in a myograph (Danish Myo Technology, Aarhus, Denmark) for isometric tension recordings. The chambers of the myograph contained PSS maintained at 37°C and aerated with 95% O₂/5% CO₂. Changes in tension were recorded by PowerLab and Chart software (ADInstruments, Oxford, United Kingdom). The arteries were equilibrated for 30 minutes and normalized to passive force. Artery segments were precontracted with 10 µM methoxamine (Sigma; Copenhagen, Denmark) in the absence or presence of linopirdine (10 µM) (Sigma; Copenhagen, Denmark), before application of ECG, EGCG or EC (Sigma; Copenhagen, Denmark).

Results

Green tea extract inhibits KCNQ1/E1 and activates an endogenous oocyte Na⁺ current

EGCG is one of the major components of green tea, with the average cup containing approximately 78 mg of EGCG [25]. EGCG inhibits some voltage-gated potassium channels, such as the cardiac potassium channels human ether-a-go-go (HERG) [26] and KCNQ1/E1 (IC₅₀ of 6 and 30.1 µM, respectively) [27]. Due to the high concentration of EGCG in green tea, we hypothesized that green tea extract (GTE) would inhibit KCNQ1/E1.

Using two-electrode voltage clamp (TEVC) recording of currents expressed in *Xenopus laevis* oocytes injected with cRNA encoding KCNQ1 and KCNE1 (10 ng and 2 ng), we studied the effects on KCNQ1/E1 of 1% GTE prepared using a methanolic extraction of organic green tea (Fig. 1D, 1E). As expected, we saw inhibition (66.3 ± 8.8 % at +40 mV prepulse) with the addition of 1% GTE, which is also reflected in the tail and prepulse current analysis (Fig. 1F), with no statistically significant change in E_M (Fig. 1G).

Interestingly, a ‘hook’ was clearly present in the KCNQ1/E1 tail current at the more depolarized prepulse sweeps (0–40 mV), only in the presence of GTE (Fig. 1H). In inactivating channels, such as KCNQ1 without accessory proteins (Fig. 1I), a similar hook appears in the tail current as the membrane potential becomes more negative, causing the channel to pass through an open state when going from an inactivated state to a closed state [28]. As the inactivating property of KCNQ1 is eliminated when KCNQ1 is associated with KCNE1 [29], the appearance of a hook in the tail current was highly unusual.

Because it seemed unlikely that GTE was inducing inactivation in a non-inactivating channel [30], we next investigated the impact GTE had on endogenous oocyte currents (Fig. 1J). In the presence of 1% GTE, a negative current was induced by the more depolarizing pulses

(Fig. 1J, K). In addition, GTE shifted the unclamped oocyte E_M from approximately -30 mV to $+60$ mV, which is close to the reversal potential for Na^+ under the ionic conditions used (Fig. 1L). These data suggest that GTE activates an endogenous voltage-dependent Na^+ channel, similar to one previously observed [31–34].

Since this inward current could explain the hook induced by GTE in recordings of KCNQ1/E1 currents, we subtracted the endogenous currents from the KCNQ1/E1 currents—causing the “hook” to disappear (Fig. 1M). We still observed inhibition in the corrected prepulse and tail current (Fig. 1N).

GTE strongly activates KCNQ5 with lesser effects on KCNQ2/Q3

Since, as expected, GTE inhibited KCNQ1/E1, we next examined KCNQ5. GTE (1%) strongly hyperpolarized the voltage-dependence of KCNQ5, inducing almost 80% constitutive activation at -80 mV (Fig. 2A, B). Accordingly, GTE (1%) induced a -12 ± 1.8 mV shift in E_M of unclamped oocytes expressing KCNQ5 (Fig. 2C). KCNQ5 plays a role in regulating vascular smooth muscle tone. It is also thought to contribute to M-current production, which regulates neuronal firing [6], although KCNQ2/Q3 channels compose the main molecular correlates of the M-current [35]. GTE slightly decreased peak KCNQ2/3 current at positive potentials (Fig. 2D, E), although it increased raw and normalized tail current at -60 mV (Fig. 2F), which could explain the hyperpolarizing shift in unclamped E_M of oocytes expressing KCNQ2/Q3 (Fig. 2G). Interestingly, GTE slowed KCNQ2/3 activation, e.g., from $\tau = 44.2 \pm 0.93$ to 159.5 ± 10.6 ms at $+40$ mV (Fig. 2H).

Black tea activates KCNQ5 in the absence of milk

Black tea, typically consumed with milk, is preferred over green tea in many countries, such as United Kingdom. Black tea extract (1%, made from PG Tips brand teabags) was effective at hyperpolarizing the voltage-dependence of KCNQ5 activation with a $V_{0.5\text{activation}}$ shift of -10.7 ± 2.4 mV (Fig. 3A–C) and the E_M of cells expressing KCNQ5 shifting -11.7 ± 4.9 mV (control mean $E_M = -58.0$ mV, black tea extract addition mean $E_M = -69.7$, $p = 0.054$) (Fig. 3D). Interestingly, milk inhibited the KCNQ5 augmenting effects of black tea. Milk had no effect alone on KCNQ5 activity, but in combination with black tea resulted in KCNQ5 current inhibition (Fig. 3A–C) and depolarization of KCNQ5-expressing oocytes (Fig. 3D).

Epicatechin gallate activates KCNQ5

While effects on some Kv channels have been documented for EGCG, other compounds in tea are little explored in this respect. As mentioned above, the main catechins found in tea other than EGCG are epicatechin (EC), epigallocatechin (EGC), and epicatechin gallate (ECG) (Fig. 4A). Due to the striking effect green and black teas had on KCNQ5, but the unwanted inhibitory effects on KCNQ1/E1 that recapitulate those previously found for EGCG, we next studied the individual effects of EC, EGC, and ECG on KCNQ5. The addition of $100 \mu\text{M}$ EC yielded negligible effects on KCNQ5 current magnitude, voltage dependence (Fig. 4B, C) and unclamped E_M (Fig. 4D). EGC ($100 \mu\text{M}$) slightly increased KCNQ5 activity ($19 \pm 9\%$ at $+40$ mV) (Fig. 4E) but did not alter $V_{0.5\text{activation}}$ or unclamped E_M (Fig. 4E–G). In contrast, ECG ($100 \mu\text{M}$) robustly increased KCNQ5 activation at

negative potentials by shifting the $V_{0.5\text{activation}}$ by -17.1 ± 3.1 mV (Fig. 4H, I). Accordingly, GTE hyperpolarized the unclamped E_M by -11.0 ± 2.1 mV (Fig. 4J). Unlike whole GTE, these compounds did not induce a hook in the tail currents, suggesting these compounds also do not activate the endogenous oocyte voltage-dependent Na^+ channel.

Catechin activation of KCNQ5 is isoform-selective

Neither EC, EGC, nor ECG (all 100 μM) altered KCNQ1/E1 activity (Fig. 5A–I). To further test the specificity of ECG, the most KCNQ5-activating of the three, we quantified its effects on KCNQ2/Q3 and found it to be essentially inactive on this heteromeric neuronal channel (Fig. 6A, B). Thus, ECG in particular is a relatively isoform-specific KCNQ5 activator.

Current augmentation by ECG requires KCNQ5-R212

Unbiased *in silico* docking identified KCNQ5-R212, at the junction of S4 and the S4/S5 linker, as a predicted binding site for ECG (Fig. 7A–C). Accordingly, in contrast to effects on wild-type KCNQ5 (Fig. 4), KCNQ5-R212A channels were insensitive to ECG (100 μM), exhibiting negligible changes in current magnitude (Fig. 7D, E), $V_{0.5\text{activation}}$ (Fig. 7E) and unclamped E_M (Fig. 7F). We next assessed ECG sensitivity of KCNQ4/Q5 heteromers, which are also thought to help control arterial tone at rest. Interestingly, ECG slightly inhibited (Fig. 7G) and negative-shifted the $V_{0.5\text{activation}}$ (by -12.7 ± 0.8 mV) (Fig. 7H) of KCNQ4/5, with negligible effects on unclamped E_M (Fig. 7I). Thus, the docking and electrophysiology results suggested KCNQ5-R212 is necessary for the activation by, and possibly binding of, ECG; co-assembly with KCNQ4 reduces the efficacy of ECG on KCNQ5. These findings are summarized by comparing $V_{0.5\text{activation}}$ (Fig. 7J) and current fold-increase versus voltage (Fig. 7K).

The predicted ECG binding site, and critical residue R212, are located deep into the membrane near the intracellular face (Fig. 7B), albeit potentially accessible from the extracellular face via the retigabine/GABA binding pocket entrance between S5 and the VSD (Fig. 7L). We injected ECG into oocytes (to an intracellular concentration of approximately 100 μM) expressing KCNQ5 and recorded the effects 20 minutes post-injection compared to pre-injection currents and to water-injected controls. We did not observe KCNQ5 current augmentation from intracellular ECG or water (Fig. 7M, N); neither did either alter E_M of KCNQ5-expressing oocytes (Fig. 7O). We therefore conclude that despite the depth of KCNQ5-R212, it is most likely that ECG accesses it via the extracellular side through the retigabine/GABA binding pocket [9, 24].

Heated EGCG inhibits KCNQ1/E1 and activates KCNQ5.—Contrary to a prior report [27], we found that freshly prepared EGCG (100 μM) (solubilized at room temperature) had no effect on KCNQ1/E1 current magnitude (Fig. 8A, B); neither did it alter voltage dependence (Fig. 8C) or E_M of KCNQ1/E1-expressing oocytes (Fig. 8D). However, when EGCG was first heated to 35°C, then subsequently stored at 4°C before being returned to room temperature before use, its ability to inhibit KCNQ1/E1 at depolarized voltages was restored (Fig. 8E–G). In addition, its ability to hyperpolarize E_M of KCNQ1/E1-expressing oocytes, likely because of small increases in current at negative potential (Fig. 8G), was uncovered (Fig. 8H). Freshly made EGCG was able to increase KCNQ5 current at -80 mV

at concentrations above 1 μM (Fig. 8I, J) (maximal effect was 2.7-fold, at 10 μM), and at 100 μM shifted the voltage dependence of activation by -7.6 ± 2.5 mV (Fig. 8K) and the E_M of KCNQ5-expressing oocytes by -8.0 ± 1.9 mV (Fig. 8L). Strikingly, prior heating of EGCG to 35°C followed by storage at 4°C then returning to room temperature before recording resulted in a KCNQ5 current increase of 25-fold at -80 mV (100 μM EGCG) (Fig. 8M, N). Preheated EGCG also had greater effects than those of freshly prepared EGCG on KCNQ5 voltage-dependence of activation (Fig. 8O) (a negative shift of -11.7 ± 2.1 mV) and E_M of KCNQ5-expressing oocytes (Fig. 8P) (a negative shift of -12.0 ± 2.1 mV).

Fresh and heated EGCG have additive effects on KCNQ5 activation.—Liquid chromatography mass spectrometry (LC-MS) analysis revealed that green and black tea extracts each contained (Fig. 9A) the prominent peak at 459 Da also observed in fresh (non-heated) EGCG (Fig. 9B). The 459 Da peak disappeared upon heating of EGCG (Fig. 9C). As both green and black tea activated KCNQ5 even more effectively than heated EGCG (Fig. 2, 3,8), we hypothesized that rather than the fresh EGCG 459 Da peak impairing KCNQ5 activation, its degradation upon heating produces other compounds (or modified versions of EGCG) more effective at KCNQ5 activation and potentially additive with that of the 459 Da moiety. To test this hypothesis, we studied effects of combinations of compounds each at 10 μM . Fresh EGCG could not induce KCNQ5 activation in combination with ECG (Fig. 10A–C), while at 10 μM heated EGCG caused a -7.1 ± 1.6 mV shift in KCNQ5 activation voltage dependence (Fig. 10D, E) and hyperpolarized E_M by -8.7 ± 2.5 mV (Fig. 10F). Strikingly, the combination of heated and fresh EGCG produced larger shifts, in both KCNQ5 activation voltage dependence (-10.4 ± 1.7 mV) (Fig. 10G, H) and E_M (-14.2 ± 2.0 mV) (Fig. 10I). Further addition of ECG produced mixed effects and less of a hyperpolarizing shift (Fig. 10J–L). The results suggest that the fresh EGCG 459 Da moiety is not the most effective EGCG moiety with respect to KCNQ5 activation, but it does not impair KCNQ5 activation and may synergize with other EGCG moieties present in tea extract to enhance KCNQ5 activation. Further, it is possible that one or more of these moieties may compete with ECG for a KCNQ5 binding site.

ECG and EGCG KCNQ-dependently relax rat mesenteric arteries

As KCNQ5 is expressed in vascular smooth muscle cells and plays a role in regulating vascular tone, we studied the effects of tea catechins on *ex vivo* segments of rat mesenteric arterial tone under isometric tension at 37°C in the absence or presence of the relatively KCNQ-specific inhibitor linopirdine. ECG relaxed arterial segments pre-contracted with methoxamine. This relaxation was partially linopirdine-sensitive (Fig. 11A). EGCG was even more efficacious at relaxing mesenteric artery and its effects were highly linopirdine-sensitive (Fig. 11B). In contrast, and consistent with lack of effects on KCNQ5 in oocytes, epicatechin did not relax mesenteric artery segments (Fig. 11C). The EC_{50} for ECG relaxation of arteries was 3.1 ± 0.4 μM , which was shifted to 26 ± 0.1 μM by linopirdine ($n = 6$) (Fig. 11D). Quantification of EC_{50} values for EGCG in the presence of linopirdine was not possible because it eliminated the relaxation response to EGCG (illustrating the strong KCNQ-dependence of EGCG effects), but the R_{max} for EGCG relaxation of arterial segments was 64 ± 13 %, shifted to 5 ± 4 % by linopirdine. Consistent with *in vitro*

effects on KCNQ5, the myography data strongly suggested that ECG and EGCG are KCNQ-dependent vasodilators.

Discussion

Tea played a role in creating the world as we know it today. As the consumption of tea spread across the globe, it changed the areas it encountered. It was used as a status symbol, led to new trading routes, helped with religious practices, and even played a role in instigating the American Revolution [36]. With more than 2 billion people currently consuming tea daily in one form or another, it is still playing a significant role in society. Not only has tea had significant cultural and historical impacts on the world, there have also been many reported health benefits to drinking tea—dating as far back as the Shang dynasty (1766–1050 BC), during which tea leaves were used as an herbal remedy in conjunction with other forest herbs [36]. For as long as tea has been around, it has been considered to have medicinal properties. Though people have only recently started studying the science behind tea's perceived health benefits, there is a growing pool of evidence that drinking tea, especially green tea, can help with cardiovascular health and can inhibit carcinogenesis [4–7]. As exciting as these results are, the mechanism behind these health benefits has remained largely elusive.

Other commonly consumed plants that, like green and black tea [37], are known to have hypotensive properties, were also recently shown [9] to activate KCNQ5, a voltage-gated potassium channel expressed in vascular smooth muscle that regulates vascular tone. Here, we show that 1% methanol-extracted black and green teas are capable of strongly activating KCNQ5. At hyperpolarized potentials, GTE increased the tail current by nearly 20-fold and diminished the voltage-dependence of the channel. Unlike KCNQ5, KCNQ1/E1, necessary for the cardiac delayed rectifier K^+ current, was inhibited by GTE—likely due to the high concentration of EGCG in GTE. Similar to other hypotensive plants studied [9], GTE had relatively minimal effects on KCNQ2/Q3 complexes.

Interestingly, in the present study GTE shifted the unclamped, non-injected oocyte E_M by approximately 90 mV to +60 mV, close to the reversal potential for Na^+ under the ionic conditions used (Fig. 1L) and induced a negative current. These data are consistent with GTE activating an endogenous voltage-dependent Na^+ current, similar to one previously described by several different groups [31–34]. The previously described current is non-inactivating, has a shallow voltage dependence and activates at more depolarized potentials than typical voltage-dependent Na^+ channels; it is also activated during staurosporine-induced apoptosis in *Xenopus* oocytes [33]. It is blocked by the calcium channel blocker verapamil (which is known to be relatively nonselective) and by lidocaine, and is relatively insensitive to tetrodotoxin [32, 33]. The Na^+ that enters the cell through this channel is thought to be required for staurosporine-induced apoptosis, rather than it being simply activated by staurosporine but unrelated to the apoptotic process [33]. The current has been previously annotated as Na_x [34]. There is to date no known molecular correlate, and no known mammalian analog, suggesting the possibility that this channel has a unique molecular architecture, or is confined to non-mammalian chordates and possibly solely

amphibians. Future studies could determine whether GTE induces *Xenopus* oocyte apoptosis and if there is a mammalian Na_x channel with unusual sequence or structure.

As we discovered in the present study for ECG (Fig. 7), we previously found that aloperine, the KCNQ5-selective activator from the hypotensive plant *Sophora flavescens*, binds at or close to R212 [9]. This site is also required for activation of other KCNQ isoforms by botanical therapeutic compounds; E-2-dodecenal from *Coriandrum sativum* and *Eryngium foetidum* binds to the equivalent position in KCNQ2 [38], as do mallotoxin and 3-ethyl-2-hydroxy-2-cyclopenten-1-one from *Mallotus oppositifolius* in KCNQ1, and mallotoxin in KCNQ2/Q3 channels [39]. The R212 site is juxtapositioned between the voltage sensor foot and the S4-S5 linker that connects the voltage-sensing domain to the pore module in KCNQ channels. Despite this location close to the intracellular side, we found that ECG was only effective at shifting the voltage dependence of KCNQ5 activation if applied from the extracellular face, suggesting it accesses R212 from the outside of the cell. The region containing KCNQ5-R212 is highly influential in KCNQ channel gating, and regulation by the endogenous soluble lipid-derived phosphatidylinositol 4,5-bisphosphate (PIP_2) that is required for normal KCNQ activation [40]. R212 and its equivalents form part of a binding pocket that accommodates not just plant metabolites, but also endogenous mammalian metabolites and synthetic drugs such as the anticonvulsants retigabine and gabapentin, and the neurotransmitter γ -aminobutyric acid (GABA) [24, 41–44].

The polyphenols in tea leaves have multiple promising bioactive properties. The main catechins are EC, EGC, ECG, and EGCG. Of these compounds, EGCG has been the most widely studied. It has pro-oxidant properties in cancer cells, which help induce apoptosis. Additionally, EGCG has the highest antioxidant activity out of the catechins and has been shown to chelate metal ions, which can help maintain metal homeostasis in chronic diseases like diabetes, cardiovascular disease, and atherosclerosis. EGCG also was shown to inhibit KCNQ1/E1 channels, which are expressed in cardiac myocytes and epithelia, but not in vascular smooth muscle, which lacks KCNE1, and the human ether-a-go-go (hERG) channel [27]. Inhibition of these channels could be problematic as life-threatening disorders, such as congenital long QT syndrome, are often associated with dysfunction or loss-of-function mutations in these channels [45, 46], and hERG blockade by drugs can cause acquired long QT syndrome, especially when combined with loss-of-function mutations in hERG or its cardiac β subunits [47, 48]. However, EGCG also inhibits the cardiac voltage-gated sodium channel and cardiac L-type calcium channel, and did not prolong the QT interval when applied directly to isolated guinea pig hearts [27], which express similar I_{Ks} and I_{Kr} currents to those of human hearts (generated by KCNQ1/E1 and hERG/KCNE2). Thus, if the human heart is safely exposed to EGCG in the tens of micromolar range and above, it could be because of the overall balance of inhibitory effects on both excitatory and inhibitory currents, such as occurs, e.g., with the anti-arrhythmic drug, amiodarone [49, 50].

While we found that addition of cow's milk to black tea eliminated the KCNQ5 augmenting effects of black tea *in vitro* (Fig. 3), a prior study showed that black tea ingestion resulted in robust increases in plasma levels of total phenols, catechins, quercetin and kaempferol that were unaffected by addition of sem-skimmed cow's milk to the ingested tea [51]. While another study suggested that milk impairs the increased antioxidant capability of whole

blood derived from black tea [52], others found that milk did not impair this effect of black tea consumption [53]. We conclude that in our *in vitro* experiments, milk constituents bind to black tea polyphenols and prevent them from activating KCNQ5, but that when ingested, this binding would be released, e.g., in the stomach, to permit release of polyphenols such as ECG into a free state that could permit KCNQ5 activation. The overall human plasma levels of total tea-derived phenols peak at 400 μ M about an hour after a single cup of black tea [51]. Depending on how much of this constitutes ECG, EGCG and KCNQ5-active EGCG derivatives (that form at/after heating to at least 35°C as occurs during preparation or ingestion of tea), this is well within the concentration range where we see robust effects on KCNQ5 activation (e.g., Fig. 10) and vasodilation (Fig. 11). This strongly supports the contention that polyphenol activation of KCNQ5 underlies at least some of the vascular health benefits of tea.

For this study, we also examined EC, EGC and ECG. Though EC and EGC had little to no effect on the KCNQ channels tested, ECG had a striking hyperpolarizing effect on the voltage dependence of KCNQ5 activation, with minimal effects on KCNQ1/E1 and KCNQ2/Q3. Although ECG has been studied for its anticancer properties [54, 55], little work has been conducted with ECG and cardiovascular health. Our results suggest that both ECG and EGCG contribute to the hypotensive properties of tea through KCNQ5 activation, making ECG in particular (because it lacks KCNQ1/E1 and hERG inhibition) an interesting candidate for potential drug development, possibly involving medicinal chemistry approaches to optimize its safety and efficacy profiles. Future studies may also target elucidation of the molecular changes that occur in EGCG upon heating to body temperature that enhance its KCNQ5 activation efficacy (after prior heating to 35°C herein) and permit it to relax arteries (studies conducted at 37°C herein). KCNQ5 loss-of-function mutations can also lead to intellectual disability or epileptic encephalopathy [56], therefore the identification of KCNQ5 selective activators could also help drug development for these disorders. In summary, activation of the vascular and neuronal KCNQ5 potassium channel contributes significantly to vasodilation by both green and black tea. The tea polyphenols ECG and EGCG are major contributors to this effect, via hyperpolarization of the voltage dependence of KCNQ5 activation. ECG and EGCG or optimized derivatives of these compounds are candidates for future anti-hypertensive drug development.

Acknowledgements

We are grateful to Angele De Silva (University of California, Irvine) for generating mutant channel constructs. GWA thanks Ronald Abbott for countless conversations on the benefits of tea. *Camellia sinensis* foliage photo credit: AxelBoldt (Wikipedia).

All datasets and materials are available upon reasonable request.

Funding

This study was supported by the National Institutes of Health, National Institute of General Medical Sciences and National Institute of Neurological Disorders and Stroke (GM130377 to GWA; KR is supported by T32NS045540). TAJ is funded by the Lundbeck Foundation (R323-2018-3674) and SR is funded by Danmarks Frie Forskningsfond (9039-00409A) awarded to TAJ.

References

1. Graham HN: Green tea composition, consumption, and polyphenol chemistry. *Prev Med* 1992;21:334–350. [PubMed: 1614995]
2. Hodgson JM, Puddey IB, Woodman RJ, Mulder TP, Fuchs D, Scott K, et al. : Effects of black tea on blood pressure: a randomized controlled trial. *Arch Intern Med* 2012;172:186–188. [PubMed: 22271130]
3. Carloni P, Padella L, Bacchetti T, Customu C, Kay A, Damiani E: Antioxidant activity of white, green and black tea obtained from the same tea cultivar. *Food Res Int* 2013;53:900–908.
4. Yochum L, Kushi LH, Meyer K, Folsom AR: Dietary flavonoid intake and risk of cardiovascular disease in postmenopausal women. *Am J Epidemiol* 1999;149:943–949. [PubMed: 10342803]
5. Yang YC, Lu FH, Wu JS, Wu CH, Chang CJ: The protective effect of habitual tea consumption on hypertension. *Arch Intern Med* 2004;164:1534–1540. [PubMed: 15277285]
6. Sasazuki S, Kodama H, Yoshimasu K, Liu Y, Washio M, Tanaka K, et al. : Relation between green tea consumption and the severity of coronary atherosclerosis among Japanese men and women. *Ann Epidemiol* 2000;10:401–408. [PubMed: 10964006]
7. Nakachi K, Matsuyama S, Miyake S, Suganuma M, Imai K: Preventive effects of drinking green tea on cancer and cardiovascular disease: epidemiological evidence for multiple targeting prevention. *Biofactors* 2000;13:49–54. [PubMed: 11237198]
8. Legeay S, Rodier M, Fillon L, Faure S, Clere N: Epigallocatechin Gallate: A Review of Its Beneficial Properties to Prevent Metabolic Syndrome. *Nutrients* 2015;7:5443–5468. [PubMed: 26198245]
9. Manville RW, van der Horst J, Redford KE, Katz BB, Jepps TA, Abbott GW: KCNQ5 activation is a unifying molecular mechanism shared by genetically and culturally diverse botanical hypotensive folk medicines. *Proc Natl Acad Sci U S A* 2019;116:21236–21245. [PubMed: 31570602]
10. Abbott GW, Goldstein SA: Potassium channel subunits encoded by the KCNE gene family: physiology and pathophysiology of the MinK-related peptides (MiRPs). *Mol Interv* 2001;1:95–107. [PubMed: 14993329]
11. Jepps TA: Unravelling the complexities of vascular smooth muscle ion channels: Fine tuning of activity by ancillary subunits. *Pharmacol Ther* 2017;178:57–66. [PubMed: 28336473]
12. Abbott GW: Biology of the KCNQ1 potassium channel. *New J Sci* 2014;2014:26.
13. Barhanin J, Lesage F, Guillemare E, Fink M, Lazdunski M, Romey G: K(V)LQT1 and IsK (minK) proteins associate to form the I(Ks) cardiac potassium current. *Nature* 1996;384:78–80. [PubMed: 8900282]
14. Biervert C, Schroeder BC, Kubisch C, Berkovic SF, Propping P, Jentsch TJ, et al. : A potassium channel mutation in neonatal human epilepsy. *Science* 1998;279:403–406. [PubMed: 9430594]
15. Klinger F, Gould G, Boehm S, Shapiro MS: Distribution of M-channel subunits KCNQ2 and KCNQ3 in rat hippocampus. *Neuroimage* 2011;58:761–769. [PubMed: 21787867]
16. Singh NA, Charlier C, Stauffer D, DuPont BR, Leach RJ, Melis R, et al. : A novel potassium channel gene, KCNQ2, is mutated in an inherited epilepsy of newborns. *Nat Genet* 1998;18:25–29. [PubMed: 9425895]
17. Tzingounis AV, Heidenreich M, Kharkovets T, Spitzmaul G, Jensen HS, Nicoll RA, et al. : The KCNQ5 potassium channel mediates a component of the afterhyperpolarization current in mouse hippocampus. *Proc Natl Acad Sci U S A* 2010;107:10232–10237. [PubMed: 20534576]
18. Kubisch C, Schroeder BC, Friedrich T, Lutjohann B, El-Amraoui A, Marlin S, et al. : KCNQ4, a novel potassium channel expressed in sensory outer hair cells, is mutated in dominant deafness. *Cell* 1999;96:437–446. [PubMed: 10025409]
19. Yeung SY, Pucovsky V, Moffatt JD, Saldanha L, Schwake M, Ohya S, et al. : Molecular expression and pharmacological identification of a role for K(v)7 channels in murine vascular reactivity. *Br J Pharmacol* 2007;151:758–770. [PubMed: 17519950]
20. Stott JB, Jepps TA, Greenwood IA: K(V)7 potassium channels: a new therapeutic target in smooth muscle disorders. *Drug Discov Today* 2014;19:413–424. [PubMed: 24333708]

21. Jepps TA, Olesen SP, Greenwood IA: One man's side effect is another man's therapeutic opportunity: targeting Kv7 channels in smooth muscle disorders. *Br J Pharmacol* 2013;168:19–27. [PubMed: 22880633]
22. Grosdidier A, Zoete V, Michielin O: SwissDock, a protein-small molecule docking web service based on EADock DSS. *Nucleic Acids Res* 2011;39:W270–277. [PubMed: 21624888]
23. Grosdidier A, Zoete V, Michielin O: Fast docking using the CHARMM force field with EADock DSS. *J Comput Chem* 2011;32:2149–2159. [PubMed: 21541955]
24. Manville RW, Papanikolaou M, Abbott GW: Direct neurotransmitter activation of voltage-gated potassium channels. *Nat Commun* 2018;9:1847. [PubMed: 29748663]
25. Balentine DA, Bouwens LCM: The chemistry of tea flavonoids. *Crit Rev Food Sci Nutr* 2009;37:693–704.
26. Kelemen K, Kiesecker C, Zitron E, Bauer A, Scholz E, Bloehs R, et al. : Green tea flavonoid epigallocatechin-3-gallate (EGCG) inhibits cardiac hERG potassium channels. *Biochem Biophys Res Commun* 2007;364:429–435. [PubMed: 17961513]
27. Kang J, Cheng H, Ji J, Incardona J, Rampe D: In vitro electrocardiographic and cardiac ion channel effects of (–)-epigallocatechin-3-gallate, the main catechin of green tea. *J Pharmacol Exp Ther* 2010;334:619–626. [PubMed: 20484151]
28. Pusch M, Magrassi R, Wollnik B, Conti F: Activation and inactivation of homomeric KvLQT1 potassium channels. *Biophys J* 1998;75:785–792. [PubMed: 9675180]
29. Tristani-Firouzi M, Sanguinetti MC: Voltage-dependent inactivation of the human K⁺ channel KvLQT1 is eliminated by association with minimal K⁺ channel (minK) subunits. *J Physiol* 1998;510:37–45. [PubMed: 9625865]
30. Redford KE, Abbott GW: The ubiquitous flavonoid quercetin is an atypical KCNQ potassium channel activator. *Commun Biol* 2020;3:356. [PubMed: 32641720]
31. Baud C, Kado RT, Marcher K: Sodium channels induced by depolarization of the *Xenopus laevis* oocyte. *Proc Natl Acad Sci U S A* 1982;79:3188–3192. [PubMed: 6285341]
32. Charpentier G: Effect of lidocaine on the slow Na⁺ channels of *Xenopus* oocytes. *Gen Physiol Biophys* 2002;21:355–365. [PubMed: 12693709]
33. Englund UH, Gertow J, Kagedal K, Elinder F: A voltage dependent non-inactivating Na⁺ channel activated during apoptosis in *Xenopus* oocytes. *PLoS One* 2014;9:e88381. [PubMed: 24586320]
34. Vasilyev A, Indyk E, Rakowski RF: Properties of a sodium channel (Na(x)) activated by strong depolarization of *Xenopus* oocytes. *J Membr Biol* 2002;185:237–247. [PubMed: 11891581]
35. Wang HS, Pan Z, Shi W, Brown BS, Wymore RS, Cohen IS, et al. : KCNQ2 and KCNQ3 potassium channel subunits: molecular correlates of the M-channel. *Science* 1998;282:1890–1893. [PubMed: 9836639]
36. Heiss ML: *The story of tea a cultural history and drinking guide*. Ten Speed Press, 2007.
37. Duthie GG, Duthie SJ, Kyle JA: Plant polyphenols in cancer and heart disease: implications as nutritional antioxidants. *Nutr Res Rev* 2000;13:79–106. [PubMed: 19087434]
38. Manville RW, Abbott GW: Cilantro leaf harbors a potent potassium channel-activating anticonvulsant. *FASEB J* 2019;33:11349–11363. [PubMed: 31311306]
39. De Silva AM, Manville RW, Abbott GW: Deconstruction of an African folk medicine uncovers a novel molecular strategy for therapeutic potassium channel activation. *Sci Adv* 2018;4:eav0824. [PubMed: 30443601]
40. Abbott GW: KCNQs: Ligand- and Voltage-Gated Potassium Channels. *Front Physiol* 2020;11:583. [PubMed: 32655402]
41. Manville RW, Abbott GW: Gabapentin Is a Potent Activator of KCNQ3 and KCNQ5 Potassium Channels. *Mol Pharmacol* 2018;94:1155–1163. [PubMed: 30021858]
42. Manville RW, Abbott GW: In silico re-engineering of a neurotransmitter to activate KCNQ potassium channels in an isoform-specific manner. *Commun Biol* 2019;2:401. [PubMed: 31701029]
43. Manville RW, Papanikolaou M, Abbott GW: M-Channel Activation Contributes to the Anticonvulsant Action of the Ketone Body beta-Hydroxybutyrate. *J Pharmacol Exp Ther* 2020;372:148–156. [PubMed: 31757819]

44. Wuttke TV, Seebohm G, Bail S, Maljevic S, Lerche H: The new anticonvulsant retigabine favors voltage-dependent opening of the Kv7.2 (KCNQ2) channel by binding to its activation gate. *Mol Pharmacol* 2005;67:1009–1017. [PubMed: 15662042]
45. Curran ME, Splawski I, Timothy KW, Vincent GM, Green ED, Keating MT: A molecular basis for cardiac arrhythmia: HERG mutations cause long QT syndrome. *Cell* 1995;80:795–803. [PubMed: 7889573]
46. Splawski I, Shen J, Timothy KW, Lehmann MH, Priori S, Robinson JL, et al. : Spectrum of mutations in long-QT syndrome genes. KVLQT1, HERG, SCN5A, KCNE1, and KCNE2. *Circulation* 2000;102:1178–1185. [PubMed: 10973849]
47. Abbott GW, Sesti F, Splawski I, Buck ME, Lehmann MH, Timothy KW, et al. : MiRP1 forms IKr potassium channels with HERG and is associated with cardiac arrhythmia. *Cell* 1999;97:175–187. [PubMed: 10219239]
48. Sesti F, Abbott GW, Wei J, Murray KT, Saksena S, Schwartz PJ, et al. : A common polymorphism associated with antibiotic-induced cardiac arrhythmia. *Proc Natl Acad Sci U S A* 2000;97:10613–10618. [PubMed: 10984545]
49. Punnam SR, Goyal SK, Kotaru VP, Pachika AR, Abela GS, Thakur RK: Amiodarone - a 'broad spectrum' antiarrhythmic drug. *Cardiovasc Hematol Disord Drug Targets* 2010;10:73–81. [PubMed: 20041841]
50. Wu L, Rajamani S, Shryock JC, Li H, Ruskin J, Antzelevitch C, et al. : Augmentation of late sodium current unmasks the proarrhythmic effects of amiodarone. *Cardiovasc Res* 2008;77:481–488. [PubMed: 18006430]
51. Kyle JA, Morrice PC, McNeill G, Duthie GG: Effects of infusion time and addition of milk on content and absorption of polyphenols from black tea. *J Agric Food Chem* 2007;55:4889–4894. [PubMed: 17489604]
52. Langley-Evans SC: Consumption of black tea elicits an increase in plasma antioxidant potential in humans. *Int J Food Sci Nutr* 2000;51:309–315. [PubMed: 11103296]
53. Leenen R, Roodenburg AJ, Tijburg LB, Wiseman SA: A single dose of tea with or without milk increases plasma antioxidant activity in humans. *Eur J Clin Nutr* 2000;54:87–92. [PubMed: 10694777]
54. Babich H, Nissim HA, Zuckerbraun HL: Differential in vitro cytotoxicity of (–)-epicatechin gallate (ECG) to cancer and normal cells from the human oral cavity. *Toxicology in vitro* 2005;19:231–242. [PubMed: 15649637]
55. Baek SJ, Kim JS, Jackson FR, Eling TE, McEntee MF, Lee SH: Epicatechin gallate-induced expression of NAG-1 is associated with growth inhibition and apoptosis in colon cancer cells. *Carcinogenesis* 2004;25:2425–2432. [PubMed: 15308587]
56. Lehman A, Thouta S, Mancini GMS, Naidu S, van Slegtenhorst M, McWalter K, et al. : Loss-of-Function and Gain-of-Function Mutations in KCNQ5 Cause Intellectual Disability or Epileptic Encephalopathy. *Am J Hum Genet* 2017;101:65–74. [PubMed: 28669405]

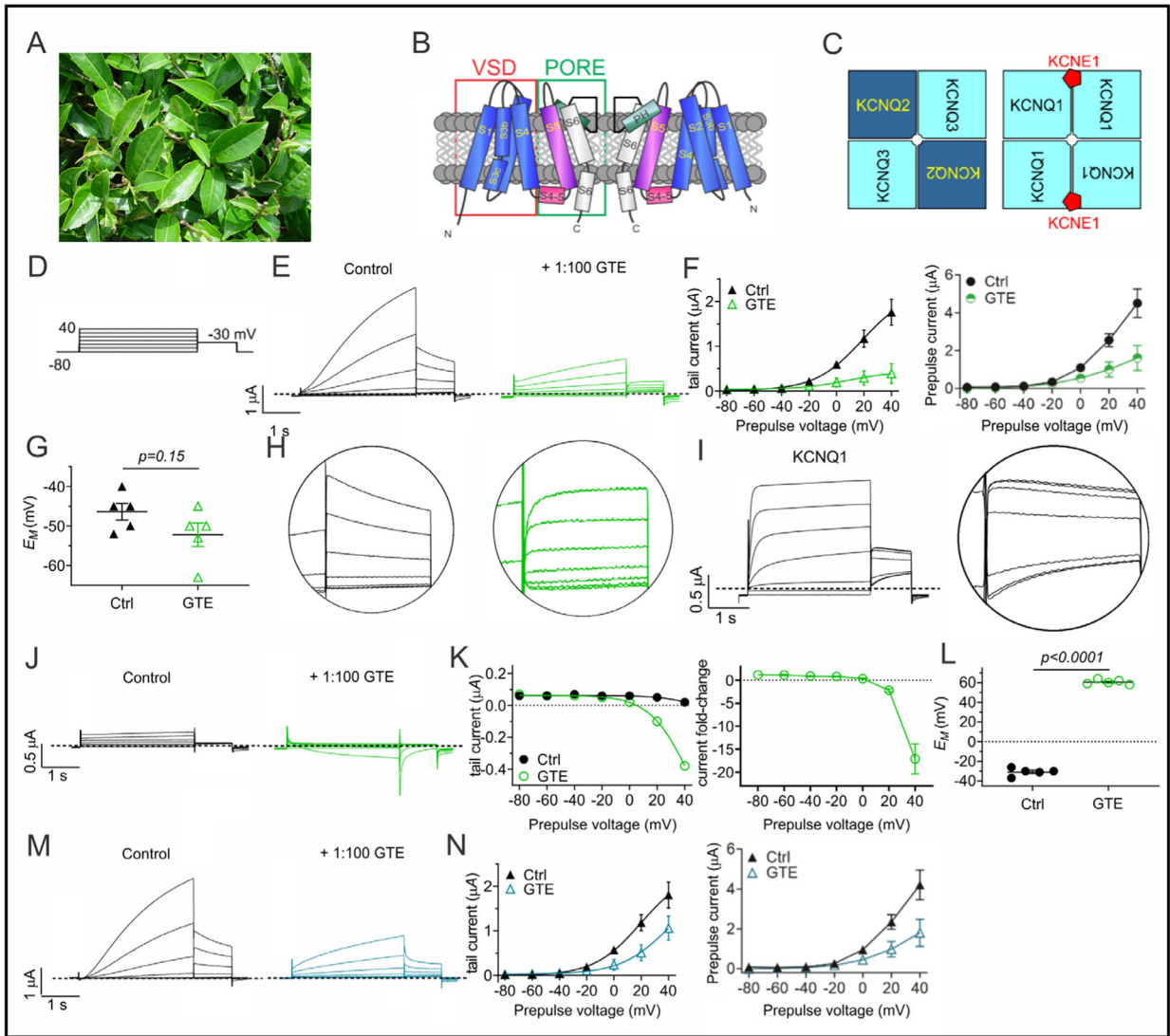


Fig. 1.

Green tea extract inhibits KCNQ1/E1 channels. All error bars indicate SEM. A: Image of the tea producing plant, *Camellia sinensis*. B: Topological representation of a Kv channel showing two of the four α subunits that comprise a channel. PH, pore helix; VSD, voltage sensing domain. C: Schematic of heteromeric composition of KCNQ2/KCNQ3 (left) and KCNQ1/KCNE1 (right) channels. D: Voltage protocol used throughout the study (20 mV prepulse increments). E: Mean TEVC current traces for KCNQ1/E1 cRNA-injected *Xenopus* oocytes (10 ng/ 2 ng) as indicated, in the absence (Control) or presence of 1% green tea extract (GTE) ($n = 5$). Dashed line here and throughout indicates the zero-current level. F: Left, mean tail current; right, mean prepulse peak current versus prepulse voltages for traces as in E ($n = 5$). G: Scatter plot of unclamped membrane potential (E_M) for cells as in E ($n = 5$). Statistical analyses by two-way ANOVA. H: Magnified mean tail currents from E (left, control; right, green tea extract). I: Mean TEVC current trace for KCNQ1 (left), with mean tail current magnified (right). J: Mean TEVC current traces for uninjected oocytes in the absence (Control) or presence of GTE. K: Left, mean tail current; right, mean tail current

fold-change versus prepulse voltage for traces as in J (n = 5). L: Scatter plot of unclamped membrane potential (E_M) for cells as in E (n = 5). Statistical analyses by two-way ANOVA. M: Mean TEVC currents from uninjected oocytes (J) subtracted from mean KCNQ1/E1 currents (E). N: Left, mean tail current; right, mean prepulse current versus prepulse voltage for traces as in M (n = 5).

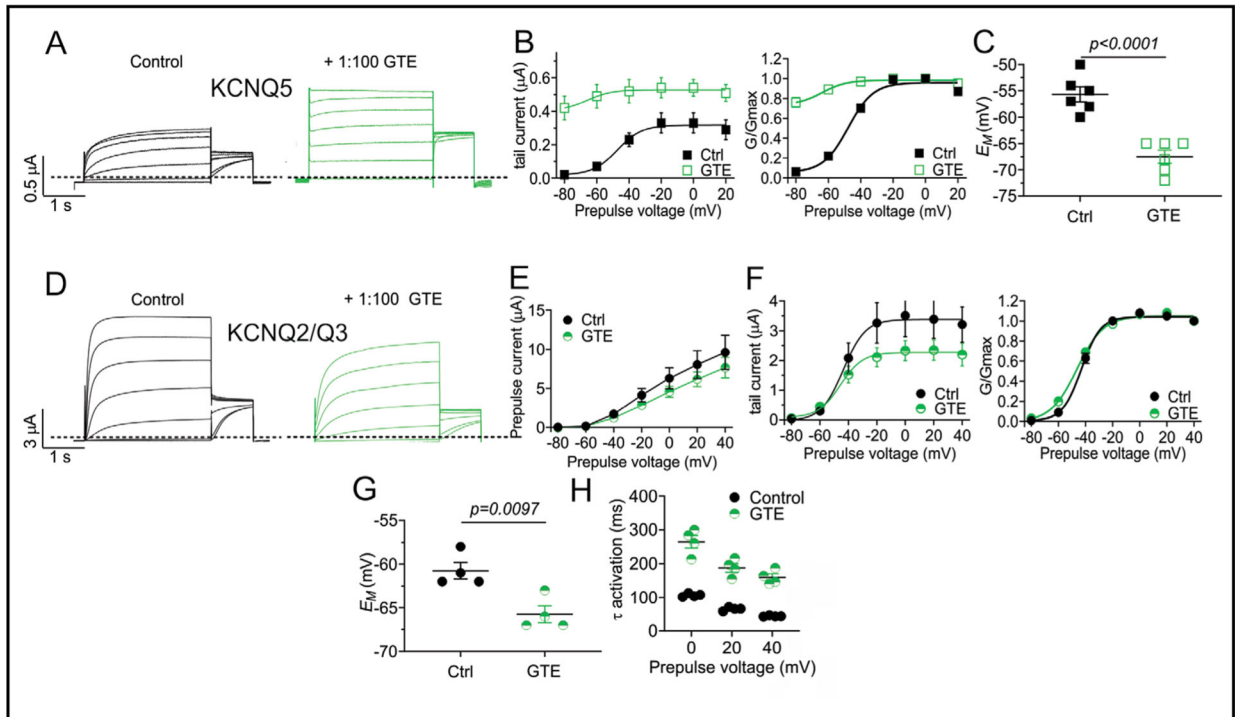


Fig. 2.

Green tea activates KCNQ5, with mixed effects on KCNQ2/Q3. All error bars indicate SEM. A: Mean KCNQ5 current traces in the absence (Control) and presence of 1% green tea extract (GTE) ($n = 5$). B: Left, mean tail current; right, mean normalized tail current (G/G_{max}) versus prepulse voltage for traces as in A ($n = 5$). C: Scatter plot of unclamped membrane potential (E_M) for cells as in A ($n = 5$). Statistical analyses by two-way ANOVA. D: Mean KCNQ2/KCNQ3 traces in the absence and presence of 1% GTE ($n = 4$). E: Mean prepulse currents versus prepulse voltages for traces as in D ($n = 4$). F: Left, mean tail current; right, mean normalized tail current (G/G_{max}) versus prepulse voltage for traces as in D ($n = 4$). G: Scatter plot of unclamped membrane potential (E_M) for cells as in D ($n = 4$). Statistical analyses by two-way ANOVA. H: Scatter plot of activation rate τ values in the absence and presence of 1% GTE for 0, 20, and 40 mV for traces as in D ($n = 4$).

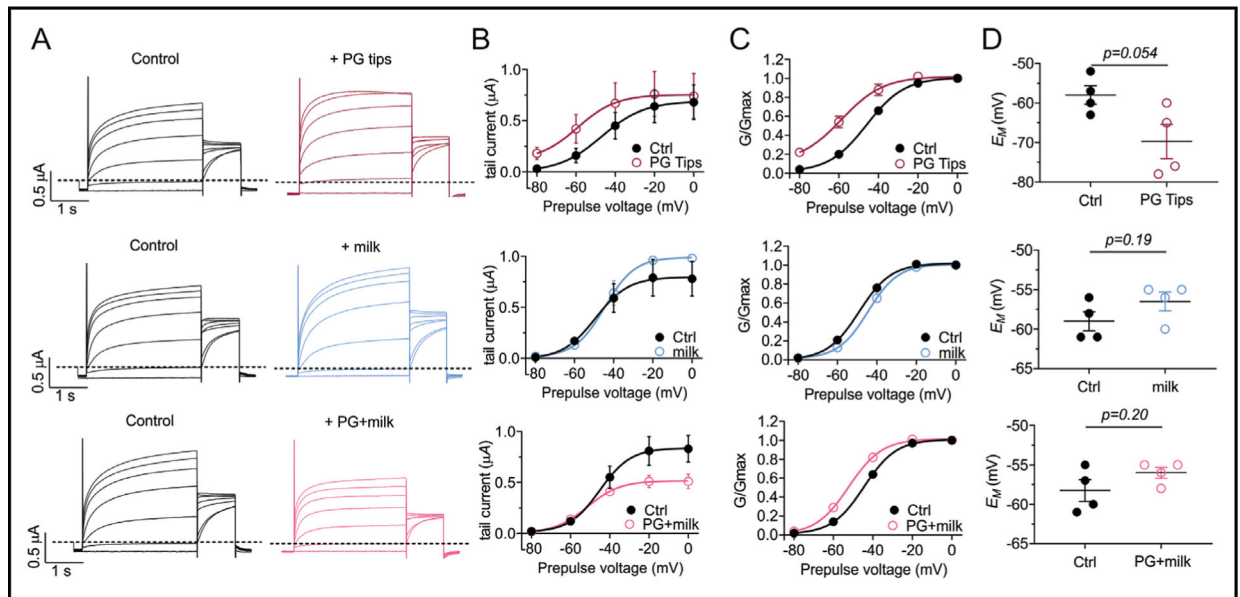


Fig. 3.

Black tea activates KCNQ5, an effect inhibited by milk. All error bars indicate SEM. A: Mean KCNQ5 current traces in the absence (Control) and presence of 1% extract of PG Tips brand black tea and/or milk ($n = 4-5$). B: Mean tail current versus prepulse voltage for traces as in A ($n = 4-5$). C: Mean normalized tail current (G/G_{max}) versus prepulse voltage for traces as in A ($n = 4-5$). D: Scatter plot of unclamped membrane potential (E_M) for cells as in A ($n = 4-5$). Statistical analyses by two-way ANOVA.

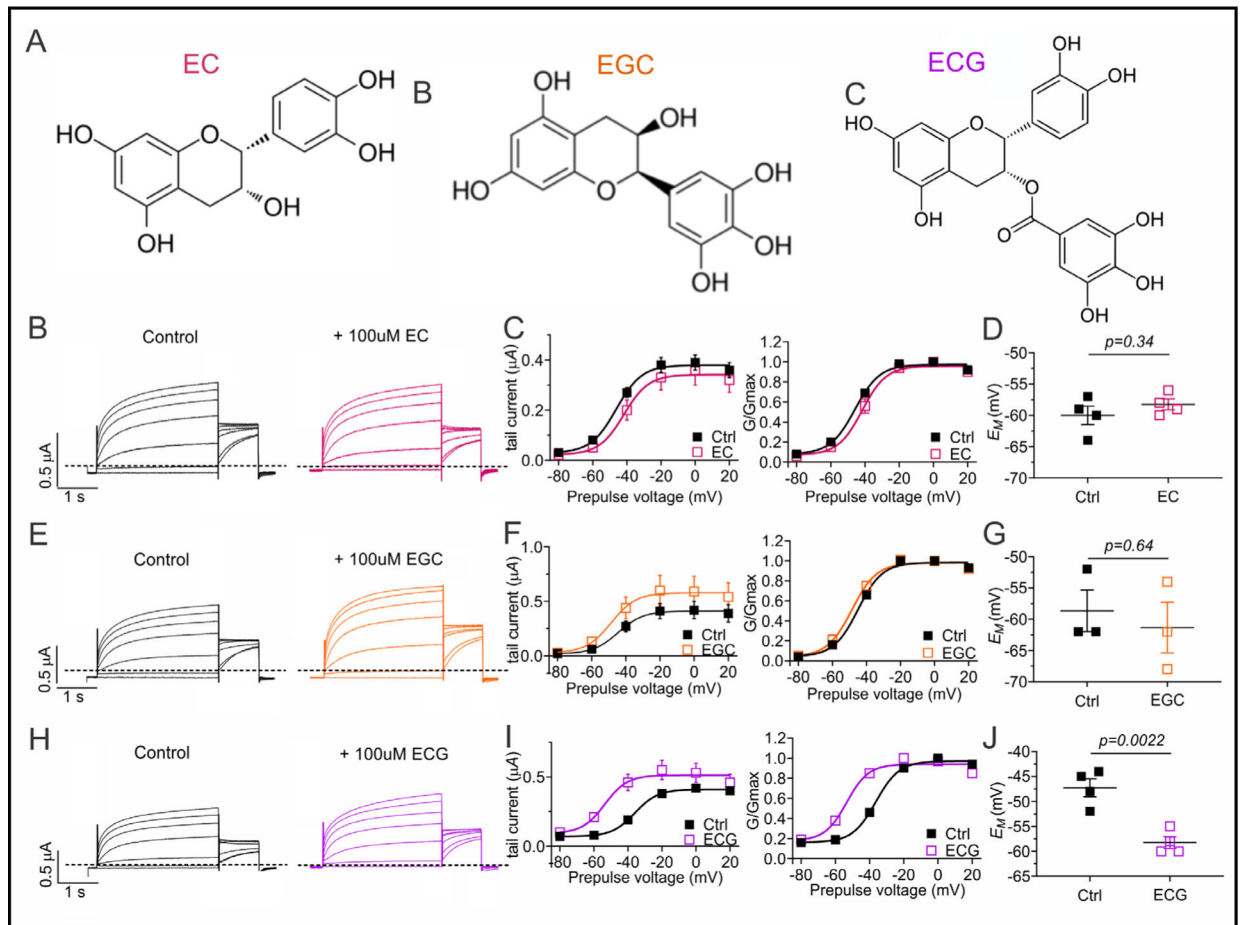


Fig. 4.

Epicatechin gallate activates KCNQ5 channels. All error bars indicate SEM. A: Chemical structures of compounds used in this study, from left to right: (-)-epicatechin (EC), (-)-epigallocatechin (EGC), and (-)-epicatechin gallate (ECG). B: Mean KCNQ5 traces in the absence (Control) and presence of 100 µM EC (n = 4). C: Left, mean tail current; right, mean normalized tail current (G/Gmax) versus prepulse voltage for traces as in B (n = 4). D: Scatter plot of unclamped membrane potential (E_M) for cells as in B (n = 4). Statistical analyses by two-way ANOVA. E: Mean KCNQ5 traces in the absence (Control) and presence of 100 µM EGC (n = 3). F: Left, mean tail current; right, mean normalized tail current (G/Gmax) versus prepulse voltage for traces as in E (n = 3). G: Scatter plot of unclamped membrane potential (E_M) for cells as in E (n = 3). Statistical analyses by two-way ANOVA. H: Mean KCNQ5 traces in the absence (Control) and presence of 100 µM ECG (n = 4). I: Left, mean tail current; right, mean normalized tail current (G/Gmax) versus prepulse voltage for traces as in H (n = 4). J: Scatter plot of unclamped membrane potential (E_M) for cells as in H (n = 4). Statistical analyses by two-way ANOVA.

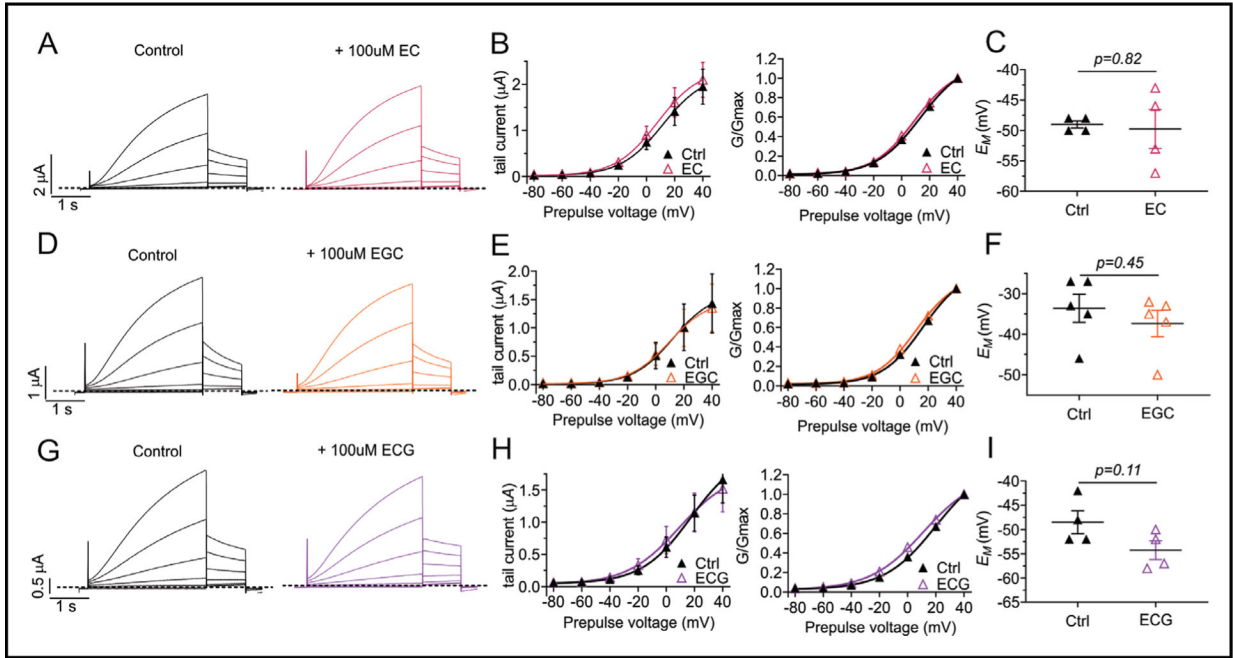


Fig. 5. EC, EGC and ECG have negligible effects on KCNQ1/E1 channels. All error bars indicate SEM. A: Mean KCNQ1/E1 traces in the absence (Control) and presence of 100 μ M EC (n = 4). B: Left, mean tail current; right, mean normalized tail current (G/Gmax) versus prepulse voltage for traces as in A (n = 4). C: Scatter plot of unclamped membrane potential (E_M) for cells as in A (n = 4). Statistical analyses by two-way ANOVA. D: Mean KCNQ1/E1 traces in the absence and presence of 100 μ M EGC (n = 5). E: Left, mean tail current; right, mean normalized tail current (G/Gmax) versus prepulse voltage for traces as in D (n = 5). F: Scatter plot of unclamped membrane potential (E_M) for cells as in D (n = 5). Statistical analyses by two-way ANOVA. G: Mean KCNQ1/E1 traces in the absence and presence of 100 μ M ECG (n = 4). H: Left, mean tail current; right, mean normalized tail current (G/Gmax) versus prepulse voltage for traces as in G (n = 4). I: Scatter plot of unclamped membrane potential (E_M) for cells as in G (n = 4). Statistical analyses by two-way ANOVA.

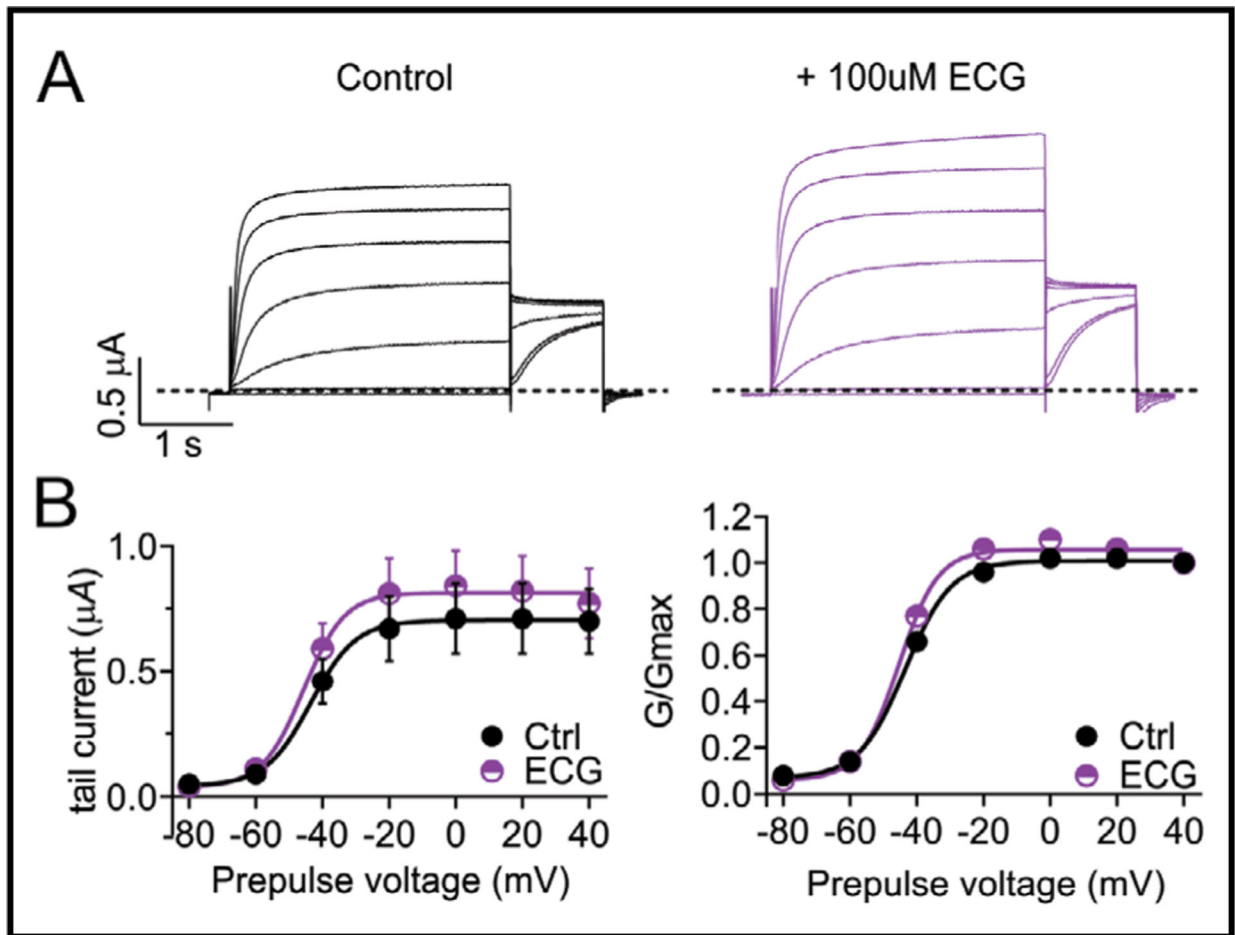


Fig. 6. Epicatechin gallate has negligible effects on KCNQ2/Q3. All error bars indicate SEM. A: Mean KCNQ2/Q3 traces in the absence (Control) and presence of 100 μ M ECG (n = 5). B: Left, mean tail current; right, mean normalized tail current (G/Gmax) versus prepulse voltage for traces as in A (n = 5).

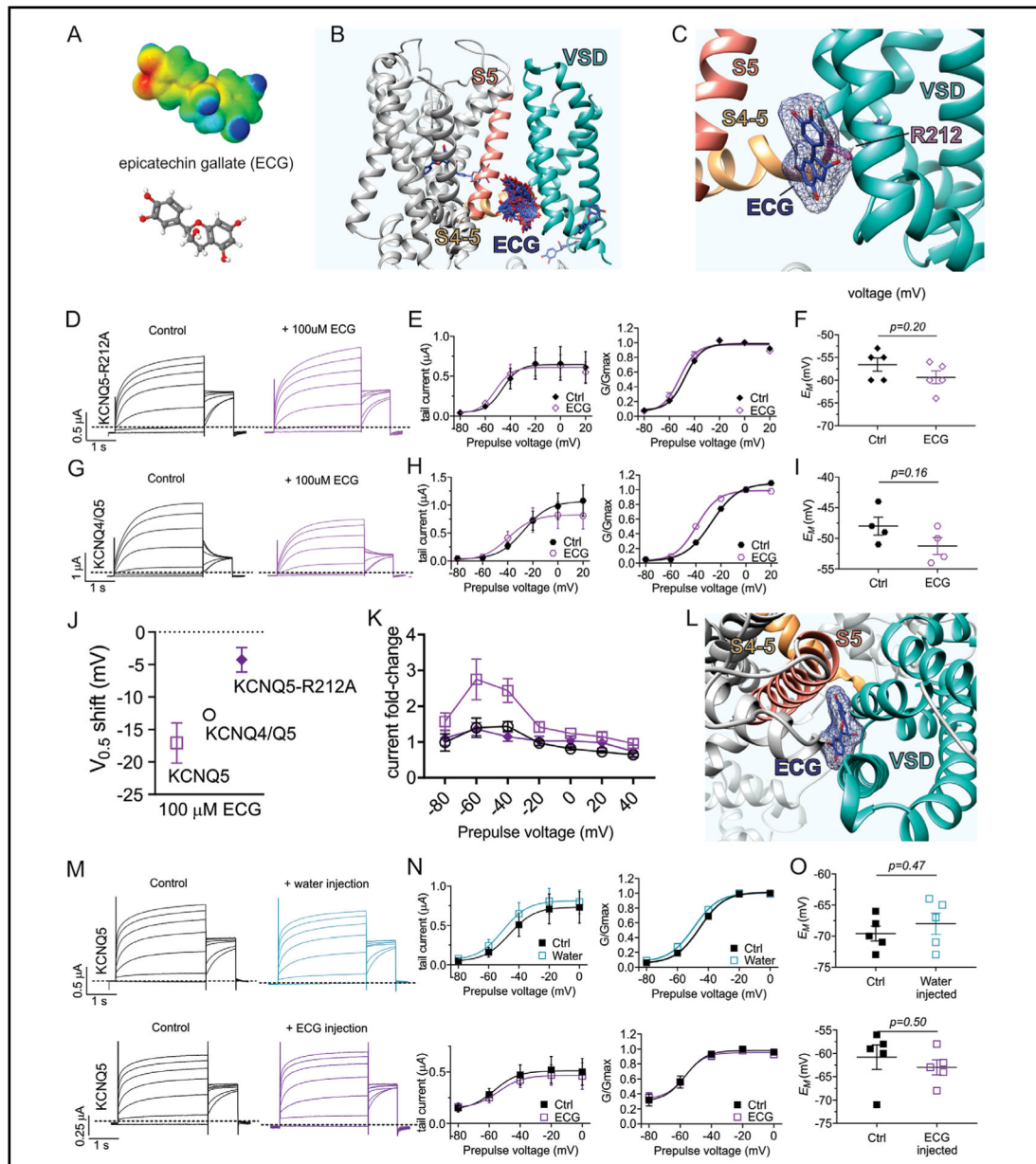


Fig. 7. Epicatechin gallate requires KCNQ5-R212 for current augmentation. All error bars indicate SEM. A: Electrostatic surface potential plot (red, negative; blue, positive) and molecular structure of epicatechin gallate (ECG). B: Unbiased results showing all predicted ECG (blue) docking poses on the transmembrane region of a neuronal KCNQ structural model based on the *Xenopus* KCNQ1 cryo-EM structure. C: Close-up of the model in panel B showing the ECG (blue) pose with the most negative predicted G score, close to the KCNQ5-R212 equivalent position (pink). D: Mean KCNQ5-R212A traces in the absence (Control) and presence of 100 μ M ECG ($n = 5$). E: Left, mean tail current; right, mean normalized tail current (G/G_{max}) versus prepulse voltage for traces as in D ($n = 5$). F: Scatter plot of unclamped membrane potential (E_M) for cells as in D ($n = 5$). Statistical

analyses by two-way ANOVA. G: Mean KCNQ4/Q5 traces in the absence (Control) and presence of 100 μ M ECG (n = 4). H: Left, mean tail current; right, mean normalized tail current (G/Gmax) versus prepulse voltage for traces as in G (n = 4). I: Scatter plot of unclamped membrane potential (E_M) for cells as in G (n = 4). Statistical analyses by two-way ANOVA. K: $V_{0.5\text{activation}}$ of KCNQ5, KCNQ4/Q5, and KCNQ5-R212A induced by 100 μ M ECG (n = 4–5). J: Tail current fold-change of KCNQ5, KCNQ4/Q5, and KCNQ5-R212A induced by 100 μ M ECG (n = 4–5). L: A view from the extracellular side of the predicted ECG binding site in panel C. M: Mean KCNQ5 traces in the absence (Control) and presence of injected ECG (50 nl, 2 mM in water) or water as indicated (n = 5). N: Left, mean tail current; right, mean normalized tail current (G/Gmax) versus prepulse voltage for traces as in M (n = 5). O: Scatter plot of unclamped membrane potential (E_M) for cells as in M (n = 5). Statistical analyses by two-way ANOVA.

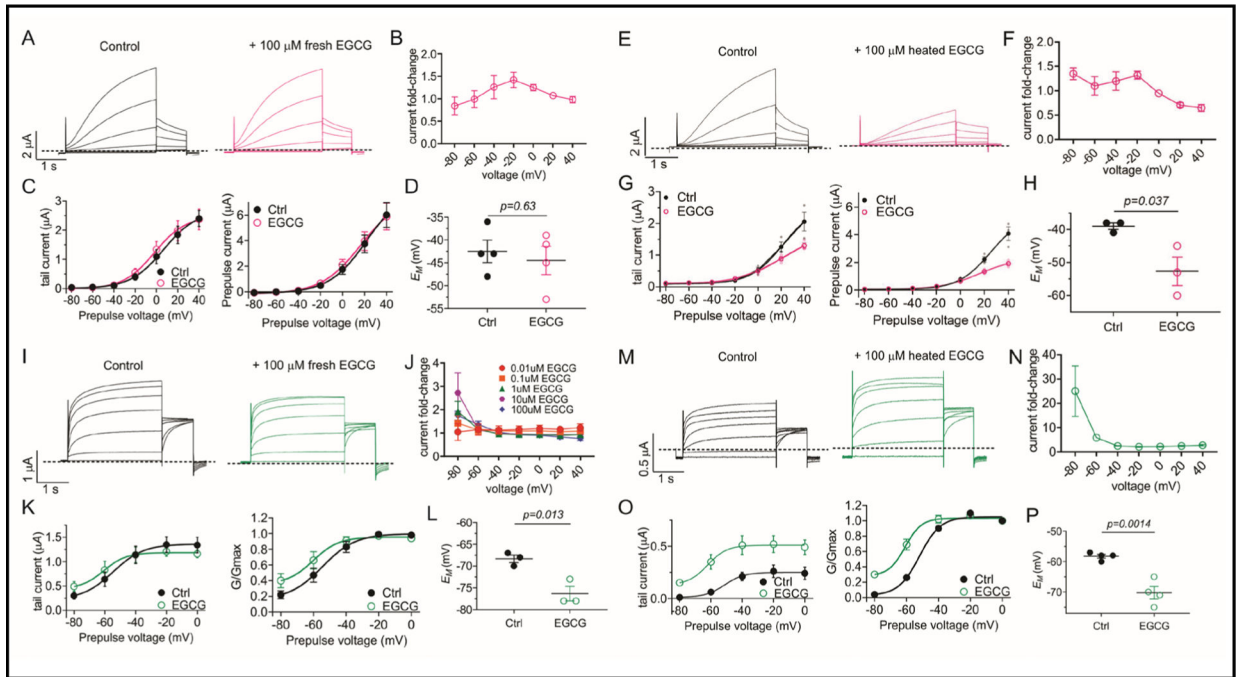


Fig. 8. Heating EGCG enables KCNQ1/E1 inhibition and KCNQ5 activation. All error bars indicate SEM. A: Mean KCNQ1/E1 traces in the absence (Control) and presence of 100 μ M fresh EGCG (n = 4). B: KCNQ1/E1 tail current fold-change versus voltage for traces as in A (n = 4). C: Left, mean tail current; right, mean prepulse current versus prepulse voltage for traces as in A (n = 4). D: Scatter plot of unclamped membrane potential (E_M) for cells as in A (n = 4). Statistical analyses by two-way ANOVA. E: Mean KCNQ1/E1 traces in the absence (Control) and presence of 100 μ M heated EGCG (n = 4). F: KCNQ1/E1 tail current fold-change versus voltage for traces as in E (n = 4). G: Left, mean tail current; right, mean prepulse current versus prepulse voltage for traces as in E (n = 4). H: Scatter plot of unclamped membrane potential (E_M) for cells as in E (n = 4). Statistical analyses by two-way ANOVA. I: Mean KCNQ5 traces in the absence (Control) and presence of 100 μ M fresh EGCG (n = 4). J: KCNQ5 tail current fold-change versus voltage for traces as in I, for a range of fresh EGCG concentrations (n = 4). K: Left, mean tail current; right, mean normalized tail current (G/Gmax) versus prepulse voltage for traces as in I (n = 4). L: Scatter plot of unclamped membrane potential (E_M) for cells as in I (n = 4). Statistical analyses by two-way ANOVA. M: Mean KCNQ5 traces in the absence (Control) and presence of 100 μ M heated EGCG (n = 4). N: KCNQ5 tail current fold-change versus voltage for traces as in M (n = 4). O: Left, mean tail current; right, mean normalized tail current (G/Gmax) versus prepulse voltage for traces as in M (n = 4). P: Scatter plot of unclamped membrane potential (E_M) for cells as in M (n = 4). Statistical analyses by two-way ANOVA.

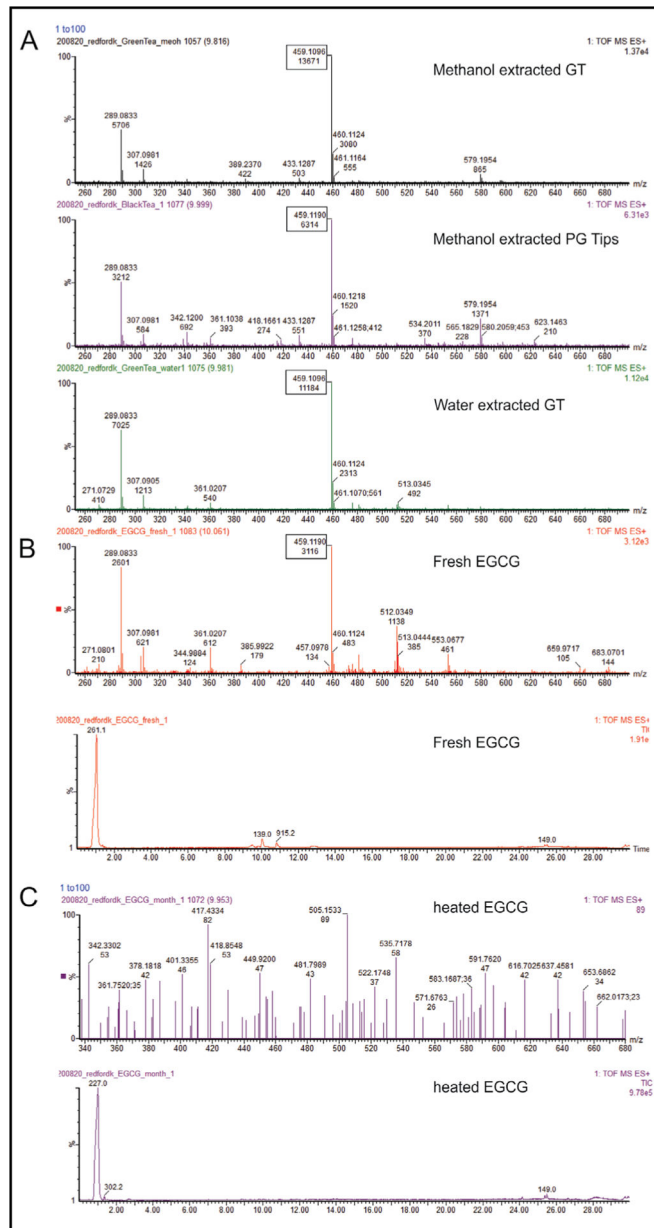
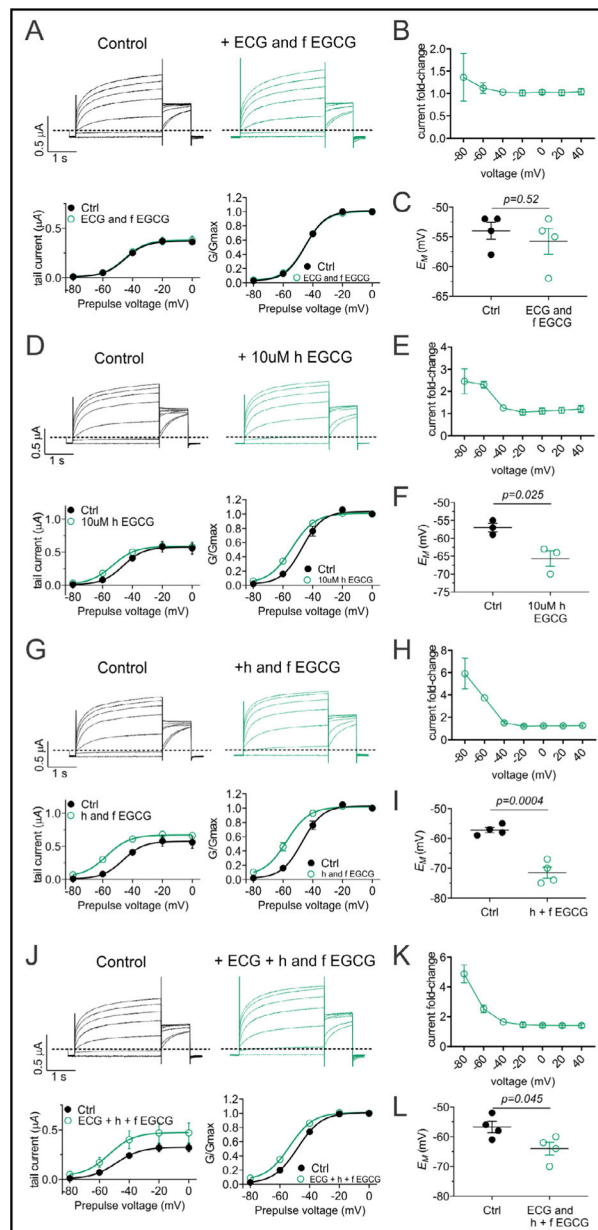


Fig. 9. LC-MS analysis of tea, fresh and heated EGCG. **A:** LC-MS mass fragmentation traces of green tea and PG Tips black tea extracts as indicated. EGCG peak boxed. **B:** LC-MS traces of fresh EGCG; lower, main peaks versus time; upper, mass fragmentation showing mass/charge (m/z). Main EGCG peak boxed. **C:** LC-MS traces of heated EGCG; lower, main peaks versus time; upper, mass fragmentation showing mass/charge (m/z).

**Fig. 10.**

Fresh and heated EGCG have additive effects on KCNQ5 activation. All error bars indicate SEM. A: Mean KCNQ5 traces, tail current and normalized tail current (G/G_{max}) versus prepulse voltage in the absence (Control) and presence of ECG + fresh (f) EGCG (each 10 μ M) ($n = 4$). B: KCNQ5 current fold-change versus voltage for traces as in D ($n = 4$). C: Scatter plot of unclamped membrane potential (E_M) for cells as in D ($n = 4$). Statistical analyses by two-way ANOVA. D: Mean KCNQ5 traces, tail current and normalized tail current (G/G_{max}) versus prepulse voltage in the absence (Control) and presence of 10 μ M heated (h) ECG ($n = 3$). E: KCNQ5 current fold-change versus voltage for traces as in G ($n = 3$). F: Scatter plot of unclamped membrane potential (E_M) for cells as in G ($n = 3$). Statistical analyses by two-way ANOVA. G: Mean KCNQ5 traces, tail current and

normalized tail current (G/G_{max}) versus prepulse voltage in the absence (Control) and presence of 10 μM each heated (h) + fresh (f) ECG ($n = 3$). H: KCNQ5 current fold-change versus voltage for traces as in J ($n = 4$). I: Scatter plot of unclamped membrane potential (E_M) for cells as in J ($n = 4$). Statistical analyses by two-way ANOVA. J: Mean KCNQ5 traces, tail current and normalized tail current (G/G_{max}) versus prepulse voltage in the absence (Control) and presence of 10 μM each ECG + heated (h) + fresh (f) ECG ($n = 4$). K: KCNQ5 current fold-change versus voltage for traces as in M ($n = 4$). L: Scatter plot of unclamped membrane potential (E_M) for cells as in M ($n = 4$). Statistical analyses by two-way ANOVA.

Author Manuscript

Author Manuscript

Author Manuscript

Author Manuscript

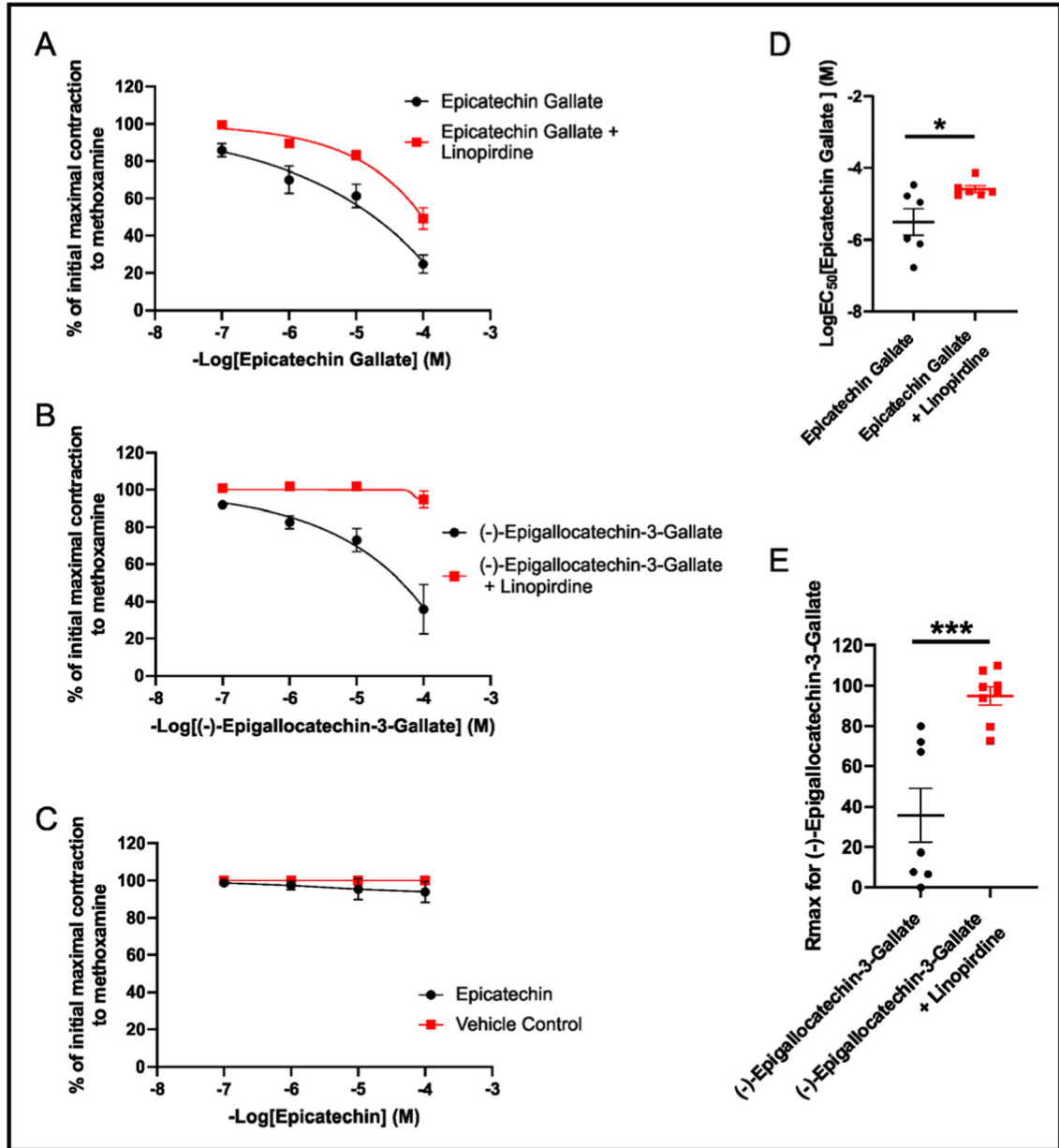


Fig. 11. ECG and EGCG are KCNQ-dependent vasorelaxants. All error bars indicate SEM. A: Concentration-response for relaxation of methoxamine-precontracted rat mesenteric artery by epicatechin gallate alone (black) or in the presence of linopirdine (red) (n = 6). B: Concentration-response for relaxation of methoxamine-precontracted rat mesenteric artery by epigallocatechin-3-gallate alone (black) or in the presence of linopirdine (red) (n = 7–8). C: Concentration-response for relaxation of methoxamine-precontracted rat mesenteric artery by epicatechin alone (black) or in the presence of linopirdine (red) (n = 4). D: Scatter plot showing epicatechin gallate LogEC_{50} values for relaxation of methoxamine-precontracted rat mesenteric artery alone or in the presence of linopirdine as indicated (n = 6). * $P < 0.05$ according to an unpaired Student’s t test. E: Scatter plot showing

epigallocatechin-3-gallate R_{\max} values for methoxamine-precontracted rat mesenteric artery alone or in the presence of linopirdine as indicated (n = 7–8). **P<0.001 according to an unpaired Student's t test.

Author Manuscript

Author Manuscript

Author Manuscript

Author Manuscript